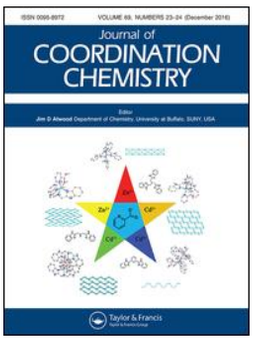

Taylor & Francis
Taylor & Francis Group

Journal of Coordination Chemistry

ISSN: 0095-8972 (Print) 1029-0389 (Online) Journal homepage: https://www.tandfonline.com/loi/gcoo20

Click chemistry electrode modification using 4-ethynylbenzyl substituted cobalt phthalocyanine for applications in electrocatalysis

Lekhetho S. Mpeta, Gertrude Fomo & Tebello Nyokong

To cite this article: Lekhetho S. Mpeta, Gertrude Fomo & Tebello Nyokong (2018) Click chemistry electrode modification using 4-ethynylbenzyl substituted cobalt phthalocyanine for applications in electrocatalysis, Journal of Coordination Chemistry, 71:10, 1623-1638, DOI: 10.1080/00958972.2018.1466118

To link to this article: https://doi.org/10.1080/00958972.2018.1466118

JOURNAL OF COORDINATION CHEMISTRY, 2018
VOL. 71, NO. 10, 1623–1638
https://doi.org/10.1080/00958972.2018.1466118

Taylor & Francis
Taylor & Francis Group

Click chemistry electrode modification using 4-ethynylbenzyl substituted cobalt phthalocyanine for applications in electrocatalysis

Lekhetho S. Mpeta, Gertrude Fomo and Tebello Nyokong

Department of Chemistry, Rhodes University, Grahamstown, South Africa

ABSTRACT

In this work, we report on the synthesis and applications of a new cobalt tetrakis 4-((4-ethynylbenzyl) oxy) phthalocyanine (**3**) for the detection of hydrazine. The glassy carbon electrode (GCE) was first grafted through diazotization, providing the GCE surface layer with azide groups. Thereafter, the 1,3-dipolar cycloaddition reaction, catalyzed by a copper(I) catalyst was used to "click" complex **3** to the grafted surface of GCE. The new platform was then characterized using cyclic voltammetry (CV), scanning electron microscopy (SEM), and X-ray photoelectron spectroscopy (XPS). This work shows that **3** is an effective sensor with sensitivity of 91.5 μA mM^{-1} and limit of detection of 3.28 μM which is a great improvement compared to other reported sensors for this analyte.

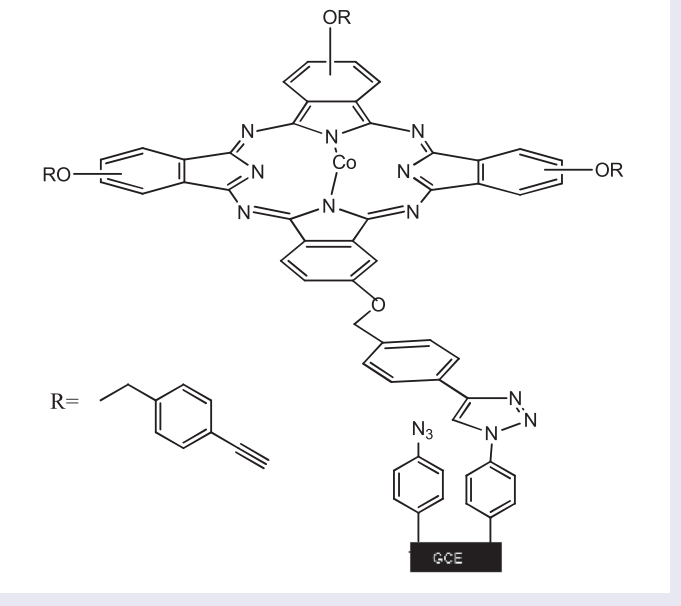

ARTICLE HISTORY
Received 16 January 2018
Accepted 4 April 2018

KEYWORDS
Click reaction; cobalt phthalocyanine; hydrazine; electrocatalysis

CONTACT Tebello Nyokong t.nyokong@ru.ac.za

1. Introduction

Metallophthalocyanines (MPcs) exhibit good electrocatalytic activity [1–4] due to accessibility of a range of oxidation states on the ring and some central metals [5]. The central metals that show electrocatalytic behavior include Co, Ni, Fe, and Mn [6–8]. MPcs have been employed as electrocatalysts for many analytes including hydrazine [8], which is of interest in this work.

Electrode modification using MPcs substituted with alkynyl groups has been reported [9–13]; however, in the reported work, the terminal alkyne was separated from the Pc ring by aliphatic chains. To the best of our knowledge, the current work is the first report of the use a substituent that has aromatic group together with aliphatic terminal alkyne group in click chemistry reaction on the electrode for analyte detection. The MPc used in this work is cobalt tetrakis 4-((4-ethynylbenzyl) oxy) phthalocyanine (**3**). This complex is substituted with four ethynylbenzyl groups which may improve the redox property of Pcs due to the presence of electron rich benzene groups when compared to the reported alkyne-terminated MPc containing aliphatic chains [10, 13] (**4** and **5** in Scheme 1).

The azide-functionalized electrode can then be "clicked" to the alkynyl substituted complex **3** through a Sharpless copper(I) catalyzed azide-alkyne cycloaddition (CuAAC) reaction resulting in a 1,2,3-triazole ring [14], the so called "click chemistry". The clicking will be preceded by electrografting of azido aniline via diazotisation [15], which results in a glassy carbon electrode (GCE) being chemically modified with azide bearing molecules. CoPc derivatives are employed since they are well known electrocatalysts for many analytes including hydrazine [8].

Hydrazine is used as a test analyte since it is a starting material for many products such as for pesticides, polymers, and pharmaceuticals [16, 17], hence its concentration levels in water must be monitored.

2. Experimental

2.1. Materials

Tetrabutylammonium tetrafluoroborate ($TBABF_4$), 4-azidoaniline hydrochloride, bromo tris (triphenylphosphine) copper(I) ($Cu(PPh_3)_3Br$), 1,8-diazobicyclo [5.4.0] undec-7-ene (DBU), hydrazine, trimethylamine, cobalt chloride, and 4-ethynylbenzyl alcohol were from Sigma-Aldrich. Dimethylformamide (DMF), acetonitrile (ACN), and acetone were purchased from Merck. Millipore water was obtained from Milli-Q Water Systems (Millipore Corp. Bedford, MA, USA). 4-Azidobenzenediazonium tetrafluoroborate was synthesized from 4-azidoaniline hydrochloride *in situ* as reported [18]. 4-Nitrophthalonitrile (**1**) was synthesized as reported [19].

2.2. Equipment

Ultraviolet–Visible (UV–Vis) absorption spectra were recorded using a Shimadzu UV-2250 spectrophotometer. Scanning electron microscopy (SEM) images of modified glassy carbon plates (Goodfellow, UK, 1 × 1 cm and 2 mm thick) were obtained using a TESCAN Vega TS 5136 LM electron microscope. Infrared (IR) spectra were recorded on a Bruker Alpha IR (100 FT-IR) spectrophotometer. Elemental analysis was done using a Vario–Elementar Microcubes ELIII, while mass spectral data were collected on a Bruker AutoFLEX III Smart-beam TOF/TOF

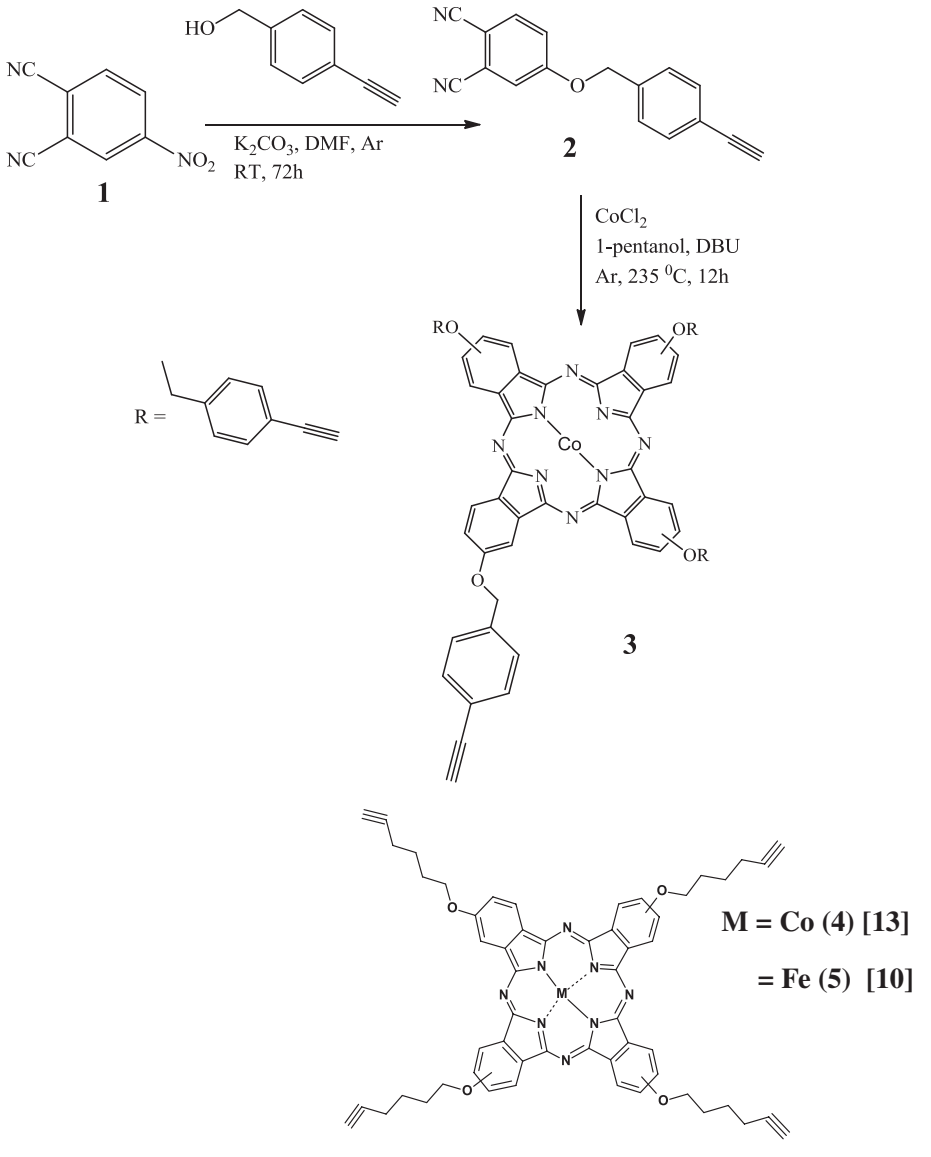

Scheme 1. Synthetic route for cobalt tetrakis 4-((4-ethynylbenzyl) oxy) phthalocyanine (**3**). The structures of complexes **4** and **5** are also shown together with references.

mass spectrophotometer using α-cyano-4-hydrocinnamic acid as the matrix in the positive ion mode.

X-ray photoelectron spectroscopy (XPS) analysis was done using an AXIS Ultra DLD, with Al (monochromatic) anode equipped with a charge neutraliser, supplied by Kratos Analytical as described [5]. The center used for the scans was at 520 eV with a width of 1205 eV, steps at 1 eV and dwell time at 100 ms. The high-resolution scans were acquired using 80 eV pass energy in slot mode. Curve fitting was performed using a Gaussian-Lorentzian peak shape after performing a linear background correction.

All electrochemical experiments (cyclic voltammetry (CV), differential pulse voltammetry (DPV) and chronoamperometry) were performed using Autolab potentiostat PGSTAT 302 electrochemical work station (driven by GPES software version 4.9).

2.3. Synthesis

2.3.1. 4-((4-Ethynylbenzyl) oxy) phthalonitrile (2), Scheme 1

4-Ethynylbenzyl alcohol (0.77 g, 5.85 mmol) and 4-nitrophthalonitrile (**1**) (1.10 g, 6.36 mmol) were dissolved in dry DMF under argon. The mixture was stirred for 15 min and then ground anhydrous potassium carbonate (0.52 g, 3.77 mmol) was added. More potassium carbonate (0.57 g, 4.40 mmol) was added after 12 h of stirring at room temperature. The mixture was stirred for a further 60 h, then it was poured into ice. The brownish product was collected by vacuum filtration and rinsed with ethanol. Yield: 0.53 g (35%). IR (cm^{-1}): 3272 (C–H, alkyne), 3090 (C–H), 1622 (C=C), 2236 (N≡C). Anal. Calcd: C 79.06%, H 3.90%, N 10.85%. Found: C 78.54%, H 3.25%, N 10.13%. ^{1}H NMR (600 MHz, $CDCl_3$) δ 8.67 (d, J = 38.5 Hz, 2H, Ar–H), 8.12 (s, 1H, Ar–H), 7.75 (d, J = 8.5 Hz, 1H, Ar–H), 7.56 (d, J = 7.1 Hz, 2H, Ar–H), 7.37 (d, J = 21.5 Hz, 1H, Ar–H), 5.18 (s, 2H, CH_2 proton), 3.15 (s, 1H, alkyne-terminated proton).

2.3.2. Cobalt tetrakis 4-((4-ethynylbenzyl) oxy) phthalocyanine (3), Scheme 1

Complex **3** was prepared by dissolving **2** (0.35 g, 2.00 mmol), cobalt chloride (0.23 g, 1.80 mmol) and DBU in 1-pentanol followed by heating at 135 °C under argon for 12 h. The mixture was then allowed to cool, and methanol was added to precipitate the product, which was further collected by centrifugation. The complex was purified by column chromatography over silica gel using chloroform as eluent. Chloroform was removed using a rotary evaporator under reduced pressure at 85 °C.

Yield: 0.2421 g (22%). IR (cm^{-1}): 3275 (C–H, alkyne), 3090 (C–H), 1622 (C=C), UV/Vis (DMF), λ_{max} nm (log ε): 668 (4.92), 604 (3.29), 340 (3.49). Anal. Calcd: C 74.79%, H 3.69%, N 10.26%. Found: C 74.60%, H 3.53%, N 10.22%. MALDI-TOF-MS (*m/z*): found = 1091.11; Cald = 1091.23 $[M]^+$.

2.4. Electrode modification via click reaction, Scheme 2

A three electrode electrochemical cell consisting of Ag|AgCl (3 M KCl) as reference electrode, a glassy carbon electrode (GCE) (geometric area of 0.071 cm^2) as the working electrode and a platinum wire as the counter electrode was used. The GCE surfaces were polished on a Buehler-felt pad using alumina (0.05 µm) and sonicated in ethanol then, in Millipore water to remove impurities and dried before use.

The bare GCE surface was first grafted by electrodeposition by scanning from +0.2 V to −1.0 V for three cycles in a solution of 0.1 mM 4-azidobenzenediazonium tetrafluoroborate salt (containing 0.01 M $TBABF_4$ in 96:4 ACN: HCl (1 M)) following methods reported [5]. The electrode was rinsed with DMF then acetone and Millipore water. Following grafting, the click reaction was performed by immersing the grafted-GCE into a solution containing 1 µM **3** in 1 mL DMF containing 2 mM $Cu(PPh_3)_3Br$ and 0.5 mL trimethylamine. The electrode was left to click for 18 h. The electrode is represented as **3**-clicked-GCE. The glassy carbon plate (GCP) surfaces used for SEM and XPS, were modified by grafting followed by clicking via the same process as applied to the GCE. Experiments were also performed where **3** was adsorbed onto the electrode without clicking. The electrode is represented as **3**-adsorbed-GCE.

3. Results and discussion

3.1. Synthesis and characterization of 3

Complex **3** (Scheme 1) was prepared from condensation of 4-((4-ethynylbenzyl) oxy) phthalonitrile (**2**) in the presence of cobalt chloride and 1-pentanol and DBU as catalyst, Scheme 1.

The presence of C–H stretch of the alkyne at 3272 cm^{-1} in the FTIR spectrum of **2** is an indication that substitution of the nitro group in 4-nitrophthalonitrile with 4-ethynylbenzyl alcohol was successful (Figure 1). The disappearance of nitrile stretch (2236 cm^{-1}) from the spectrum of **3** shows successful cyclization (Figure 1). ^1H NMR spectrum for **3** was not recorded due to the paramagnetic nature of Co. Mass spectra confirmed the formation of **3** since the anticipated molecular ion was obtained.

Figure 2 shows the UV–Vis spectrum of **3** in DMF. The intense Q band with a maximum at 659 nm is typical of metallated Pcs [20–22]. The ethynylbenzyl group results in the blue shift of the Q band compared to the aliphatic alkynyl substituted CoPc (Table 1). Complex **3** is soluble in a wide range of organic solvents including DMF, DMSO, ethanol, toluene, $CHCl_3$, *etc*.

The aggregation behavior of **3** was also investigated at different concentrations in DMF. As the concentration was increased, the intensity of absorption of the Q band also increased. The Beer-Lambert law was obeyed in the concentration range of 6 to 16 µM.

Figure 3(a) and (b) shows the cyclic and differential pulse voltammetries of **3** in DMF containing 0.1 M $TBABF_4$. The cyclic voltammogram of **3** (Figure 3(a)) showed four identifiable redox processes (I–IV). From literature [23], peaks (II) and (III) are attributed to Co(I)/Co(II) and Co(III)/Co(II), respectively, in DMF. The Co(III)/Co(II) couple is irreversible, as is often observed for this couple [24]. The rest of the peaks are ring based. Oxidation at the Pc ring occurs by successive loss of one electron from the highest occupied molecular orbital (HOMO), resulting in the formation of $[Pc^{-1}]^{\bullet+}$ and $[Pc^{0}]^{\bullet 2+}$ cation radicals. Reduction, on the

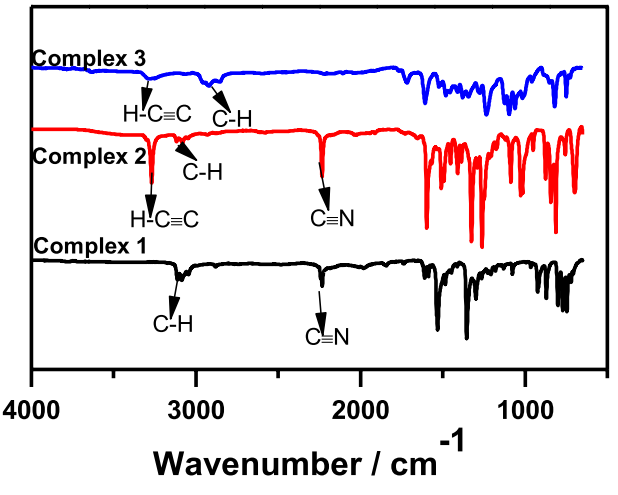

Figure 1. FTIR spectra of **1**–**3**.

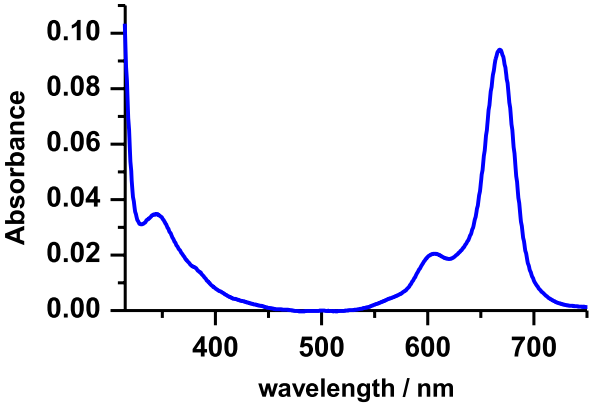

Figure 2. UV–Vis spectrum of **3** in DMF (concentration ~ 1×10^{-5}M).

Table 1. Q band absorption maxima (DMF) and electrochemical data for hydrazine oxidation on **3**-clicked-GCE with their clicked CoPc (**4**) and FePc (**5**) derivatives. Hydrazine concentration is 4, 6, and 5 (in 0.2 M NaOH) for **3**–**5**, respectively.

Complex	λ (Q band) nm	E/V hydrazine oxidation	Tafel slope (mV/dec)	Catalytic constant ($M^{-1}s^{-1}$)	Sensitivity (μA/mM)	LoD (μM)	Refs.
3[a]	659	0.54(0.58)	56(88)	8.45×10^3 (4.68×10^2)	91.53(5.46)	3.28(10.2)	This work
4	676	0.72	212	7.84×10^2	51.32	6.09	[13]
5	706	0.10	65.8	8.84×10^2	15.38	1.09	[10]

[a]Values in brackets are for **3**-adsorbed-GCE.

other hand, occurs by successive gain of electrons by the lowest unoccupied molecular orbital (LUMO) of the phthalocyanine complex, resulting in the formation of Pc (−2−n) species (where *n* = number of electrons). Since DPV is more sensitive than CV, it was used to confirm the oxidation and reduction peaks obtained on the cyclic voltammogram (Figure 3(b)).

3.2. Characterization of modified electrodes

The working electrode surface was modified as shown in Scheme 2. Although only one substituent is shown as clicked to the electrode, there is a possibility that more than one ring substituent could undergo the click reaction depending on the orientation of **3**.

3.2.1. Cyclic voltammetry (CV)

Figure 4(a) shows the grafting step where three consecutive cycles were recorded in a solution of 0.1 mM 4-azidobenzenediazonium tetrafluoroborate (containing 0.01 M $TBABF_4$ in 96:4 ACN: HCl (1 M)) at a potential window from 0.2 to −1 V. The reduction of 4-azidobenzenediazonium to diazonium radicals was observed with the reduction peak at −0.6 V on the first cycle and this peak disappeared when recording the second and third cycles, typical of electrochemical grafting process [15]. Figure 4(b) illustrates the response of the bare GCE towards 1 mM ferrocyanide solution and the expected reversible couple is obtained on the bare GCE. The grafting step resulted in the passivation of the GCE. After clicking, the electrode

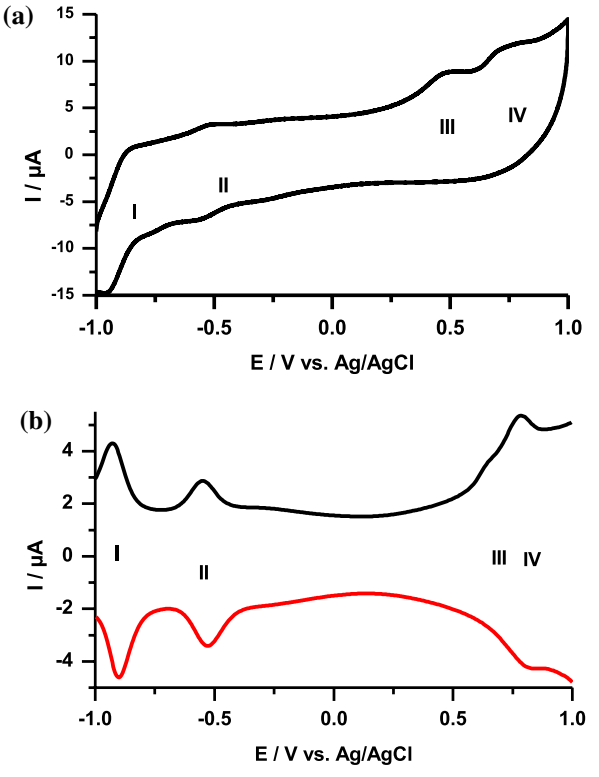

Figure 3. (a) Cyclic voltammogram (CV) and (b) differential pulse voltammogram (DPV) profiles of 1×10^{-3} M of **3** in DMF containing 0.1 M $TBABF_4$ supporting electrolyte.

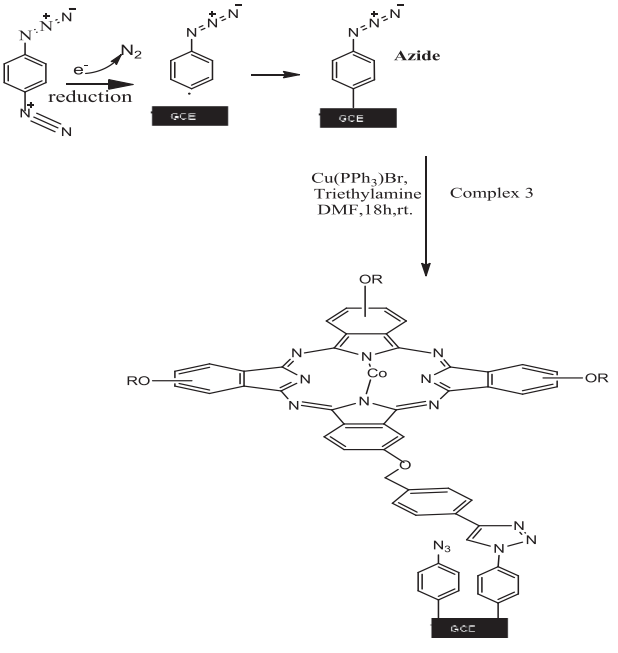

Scheme 2. Schematic illustration of grafting of GCE with azide and clicking of **3** on the grafted electrode.

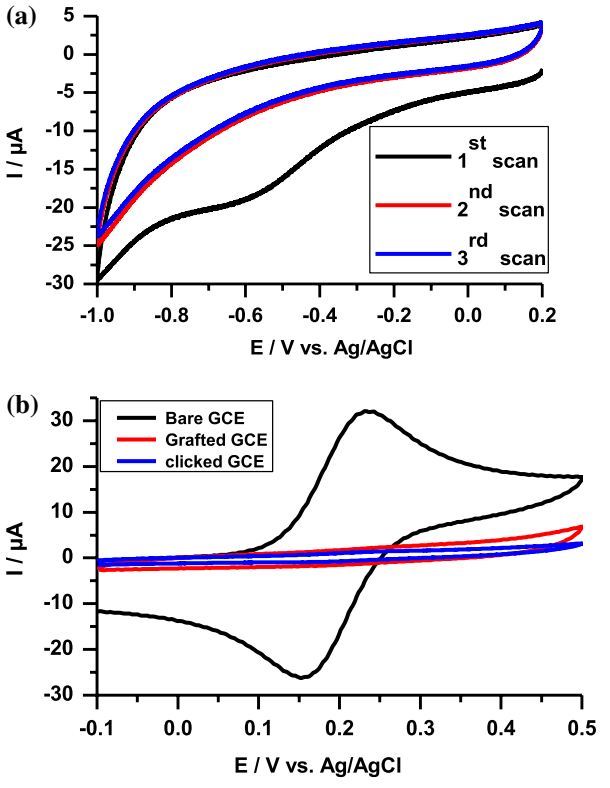

Figure 4. Cyclic voltammograms of (a) bare GCE in 0.1 mM 4-nitrobenzenediazonium tetrafluoroborate, in ACN containing 0.1 M $TBABF_4$ and (b) bare GCE, grafted GCE and **3**-clicked-GCE in 1 mM ferrocyanide solution.

was also tested in the same solution and the passivation continued. This has been observed before during click reaction [11].

3.2.2. SEM images

The SEM images of the electrodes following grafting and clicking are shown in Figure S1. On the bare glassy carbon plate Figure S1(a), the surface is homogeneous showing that the glassy carbon plate is unmodified. After grafting, Figure S1(b) the surface is not homogeneous, which is an indication that the surface is modified. In Figure S1(c), the electrode appears rougher than Figure S1(b), which is indication of further modification.

3.2.3. X-ray photoelectron spectroscopy (XPS)

XPS analysis was employed to confirm successful modification of the electrode surface via click chemistry. Figure 5(a) shows wide scan spectra for bare, grafted and clicked electrodes, showing the expected C (1s) peak at 284.9 eV. The O (1s) peak at 529.3 eV may come from air since the modification of the electrode surface was done in the open environment. The appearance of N (1s) peak at 384.6 eV on grafted and clicked GCE is an indication of a successful grafting. After the grafted GCE was clicked, the Co($2p_{3/2}$) peak is observed at the binding energy of 683.6 eV which is an indication that **3** was successfully linked to the grafted

surface. In the N (1s) high-resolution XPS spectra, the N=N peak is observed at 396.4 eV for the grafted electrode and shifts to 399.3 eV for the clicked electrodes, Figure 5(c) with an intensity decrease from 7045 cps for the former to 4386 cps for the latter. The decrease in the intensity of the azide (N=N) peak is an indication that the click reaction may have taken place. However, the presence of this peak in **3**-clicked-GCE shows that not all the azide peaks were involved in clicking. On the other hand, the presence of the N≡N peak (397.4) in the grafted electrode may indicate that not all of the 4-azidobenzenediazonium tetrafluoroborate was grafted onto the electrode or due to the fact that azide has an apparently pentavalent central nitrogen atom chain that can be represented by N=N≡N [25]. The peak is not observed following clicking confirming that it is not due to the former reason but, it is more likely due to the N=N≡N. The high resolution C(1s) spectra shows an increase in the number of peaks

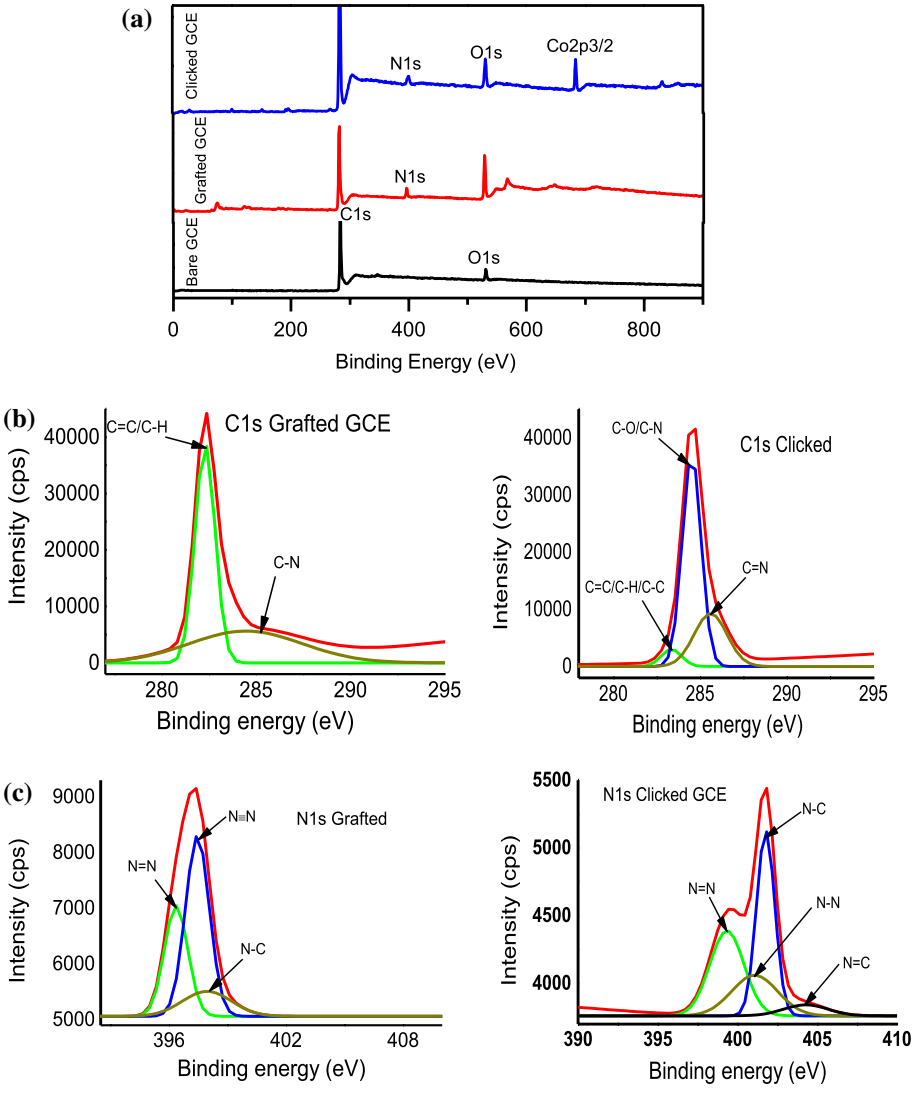

Figure 5. (a) Wide scan XPS spectra for bare, grafted and **3**-clicked-GCP. High resolution XPS spectrum of (b) C (1s) and (c) N (1s) for grafted and clicked electrodes.

following clicking with the appearance of new C=N peak at 285.7 eV in Figure 5(b), confirming the presence of the Pc on the electrode. The C-N peak appears broad in Figure 5(b). Broad C-N peaks have been observed [26]. The broadness could be due to electron delocalization or electron cloud from both benzyl and azide surrounding the carbon, while on clicked, the electron cloud is reduced on azide group.

3.3. Detection of hydrazine

3.3.1. Cyclic voltammetry

Following characterization of modified electrodes to confirm the success of each modification step, the clicked electrode was used to detect hydrazine in order to determine its electrocatalytic behavior. Hydrazine was chosen as a test analyte as it has been reported that CoPc readily oxidizes this analyte [27–29]. Figure 6 shows comparative CVs of the bare GCE, grafted GCE, **3**-clicked-GCE and **3**-adsorbed-GCE in a potential window of 0 to 0.75 V *versus* Ag/AgCl reference electrode. The results showed that the bare and the grafted electrodes were not able to sense hydrazine. In contrast, the **3**-clicked-GCE showed a defined oxidation peak at 0.54 V (Table 1) with an onset potential of 0.3 V. On the other hand, the complex **3**-adsorbed-GCE showed slightly higher oxidation potential (0.58 V) and lower peak currents, hence clicking increases the sensitivity of the electrode. The oxidation potentials obtained are more negative than for those reported for clicked CoPc (**4** in Table 1) at 0.72 V [13] in which only aliphatic substituents were used for clicking, meaning the aromatic substituent used in this work eased oxidation of hydrazine due to the presence of electron rich benzene groups as substituents resulting in low oxidation potentials. The difference between **3** and **5** (FePc) is attributed to different central metals (Table 1).

The proposed mechanism for electroxidation of hydrazine on CoPc has been reported [30, 31], Equations (1–4).

$$[\mathrm{Co(I)Pc}]^{-}_{\mathrm{surface}} \leftrightarrow [\mathrm{Co(II)Pc}]_{\mathrm{surface}} + e^{-} \tag{1}$$

$$[\mathrm{Co(II)Pc}]_{\mathrm{surface}} + \mathrm{N_2H_4} + \mathrm{OH^-} \overset{rds}{\rightarrow} [\mathit{Co}\mathrm{(I)Pc} \ldots \mathrm{N_2H_3}]^{-}_{\mathrm{surface}} + \mathrm{H_2O} \tag{2}$$

$$[\mathrm{Co(I)Pc} \ldots \mathrm{N_2H_3}]^{-}_{\mathrm{surface}} \rightarrow [\mathrm{Co(I)Pc}]^{-}_{\mathrm{surface}} + * \mathrm{N_2H_3} \tag{3}$$

$$* \mathrm{N_2H_3} + 3\mathrm{OH^-} \overset{\mathrm{fast}}{\rightarrow} \mathrm{N_2} + 3e^{-} + 3\mathrm{H_2O} \tag{4}$$

As stated in literature [30], for most CoPc complexes, oxidation of hydrazine starts at potential more positive than that of the Co(II)/(I) redox couple, indicating the catalytic species is Co(II) Pc.

3.3.2. Stability test

For practical applications of any electrochemical sensor, the stability is essential. The stability test for **3**-clicked-GCE and **3**-adsorbed-GCE were done by running 10 consecutive scans in 0.2 M NaOH supporting electrolyte solution containing 4 mM hydrazine (Figure 7). For

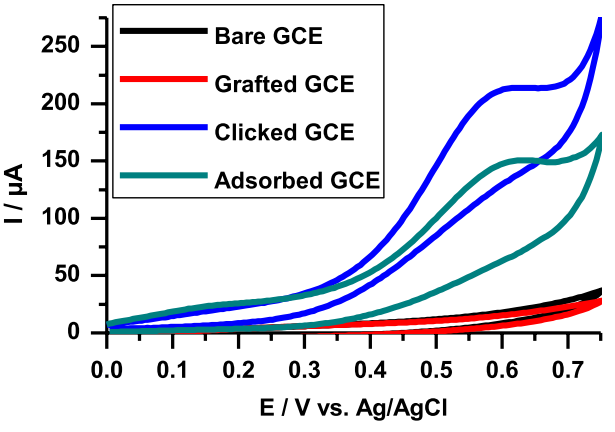

Figure 6. Cyclic voltammetry of bare, grafted, **3**-clicked-GCE, and **3**-adsorbed-GCE in 4 mM hydrazine in 0.2 M NaOH. Scan rate 100 mVs^{-1}.

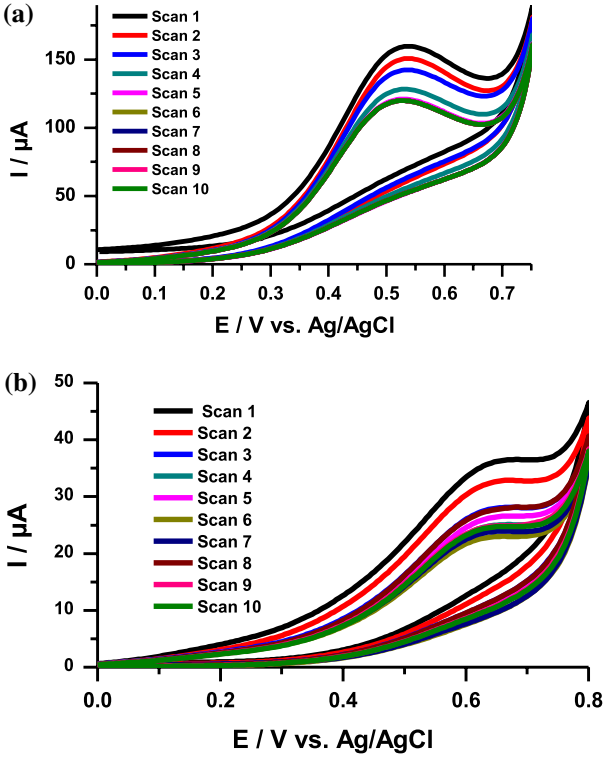

Figure 7. Cyclic voltammograms of repetitive scans (10) with (a) **3**-clicked-GCE and (b) **3**-adsorbed-GCE in 4 mM hydrazine with 0.2M NaOH.

3-clicked-GCE (a) the current decreased for the first four scans and from 5th scan the peak current and potential became stable. On the other hand, the **3**-adsorbed-GCE (b) showed a decrease in current without becoming stable for all 10 scans. Therefore, the clicked electrode

is more stable than when MPcs are adsorbed, this makes a clicked electrode more appropriate for use in sensing.

3.3.3. Kinetic studies of hydrazine detection

Figure 8(a) shows that an increase in scan rates (10 to 75 mVs^{-1}) resulted in the hydrazine oxidation peak shifting towards more positive potentials, which is an indication of irreversibility of the redox reaction. The linear relationship of the plot of peak current against square

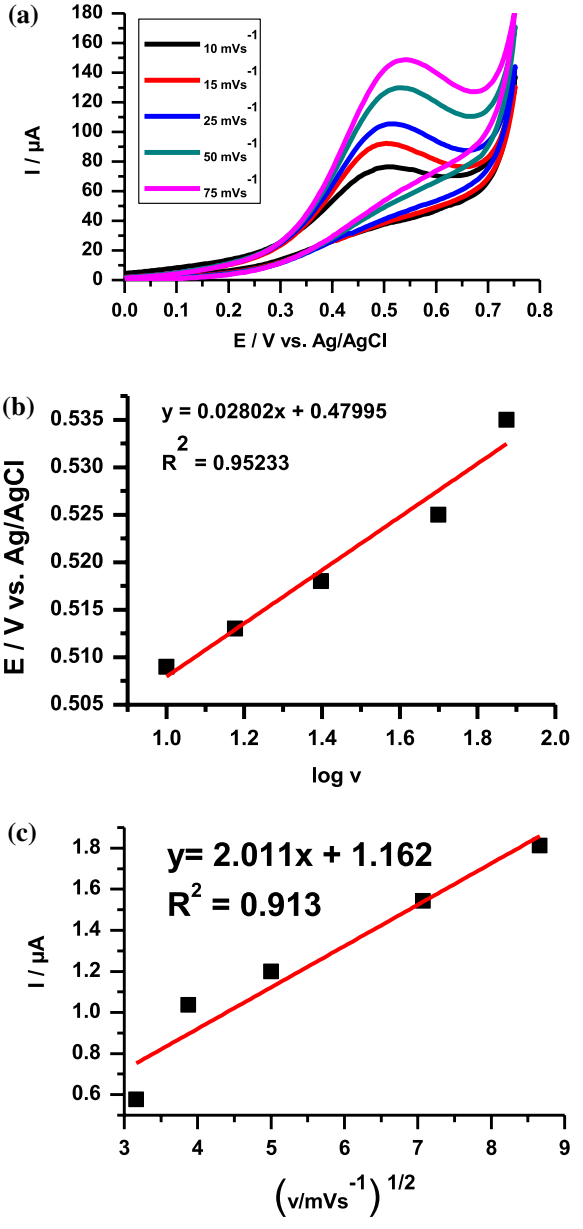

Figure 8. Cyclic voltammograms for the detection of hydrazine (in 0.2 M NaOH) at different scan rates (a), plot of oxidation peak potential *vs*. log *v* (b) and plot of peak current *vs*. square root of scan rate (c).

root of scan rate (Figure 8(c)) means that hydrazine oxidation is diffusion controlled. The relationship between peak potential and scan rate for an irreversible diffusion-controlled process is given by Equation (5) [32]:

$$E_p = \frac{b}{2}\log v + K \tag{5}$$

where E_p is the peak potential, v is the scan rate, K is a constant, and b indicates the Tafel slope. From the plot of E_p *versus* log v (Figure 8(b)), a Tafel slope (which is twice the gradient of the plot of E_p *versus* log v) of 56 mV decade^{-1} was obtained which is almost within standard range of 60–120 mV decade^{-1}. The Tafel slope for **3**-clicked-GCE is lower than that of the corresponding **4**-clicked-GCE (Table 1). A Tafel slope of near 60 mV/decade (as is the case in this work) is obtained when $\alpha = 1$, and one electron is transferred during the rate-determining step [33]. Tafel slopes higher than 120 mV/decade (as observed for **4**-clicked-GCE) have no kinetic meaning.

3.3.4. Chronoamperometry studies

The **3**-clicked-CGE was employed for chronoamperometric studies. Chronoamperogram data were used to determine the limit of detection and catalytic rate constant for the electrocatalysis of hydrazine. The limit of detection (LoD) was calculated using $3\delta/s$ (where δ is standard deviation of the blank and s is the slope of the calibration curve, Figure 9(a), insert) and was found to be 3.28 µM. Another parameter of interest that was determined was sensitivity which was 91.5 µA mM^{-1}. The LoD in the micromolar range has been reported for similar work [34], but much lower than reported for CoPc hexynyl substituent (**4**), Table 1, showing the advantage of ethynylbenzyl substituents. For **3**-adsorbed-GCE, the LoD is 10.2 µM and sensitivity is 5.45 µA mM^{-1}, hence clicking performs better than adsorption.

A higher LoD than the one for FePc containing hexynyl substituent may be due to the difference in central metal as FePc are reported to have low LoDs [35]. The catalytic rate constant (k) for the electrocatalysis of hydrazine on the **3**-clicked-CGE was determined according to the method described in the literature [36] and Equation (6):

$$\frac{I_{cat}}{I_{bla}} = y^{\frac{1}{2}}\Pi^{1/2} = \Pi^{1/2}(kC_0t)^{1/2} \tag{6}$$

where I_{cat} and I_{bla} are currents in the presence and in the absence of hydrazine, t = elapsed time in seconds and k = catalytic rate constant (M^{-1}s^{-1}). Figure 9(b) shows linear plots of (I_{cat}/I_{bla}) *versus* t$^{1/2}$ for different concentrations of hydrazine obtained from the chronoamperomogram in Figure 9(a). The slopes of these plots were plotted against the concentration of hydrazine to give the linear relationship shown in Figure 9(c) and is represented by Equation (7).

$$y = 26.5\,[\text{hydrazine}]\left(\frac{s^{-1}}{\text{mM}}\right) - 4.28s^{-1}, \qquad R^2 = 0.9701 \tag{7}$$

The slope of Figure 9(c) is equal to πk, and this gives a k value of 8.45×10^3 M^{-1}s^{-1} which is ten times faster than that reported in the literature as presented in Table 1. The k value for

adsorbed **3** of 4.68×10^2 $M^{-1}s^{-1}$ is much less than that of the clicked electrode showing the importance of clicking.

The high catalytic constant and low LoD of the **3**-clicked-CGE sensor compared to clicked complex **4** are attributed to the aromatic group that is present in the substituent in **3**. Hence the presence of the aromatic ring improves the performance of the sensor.

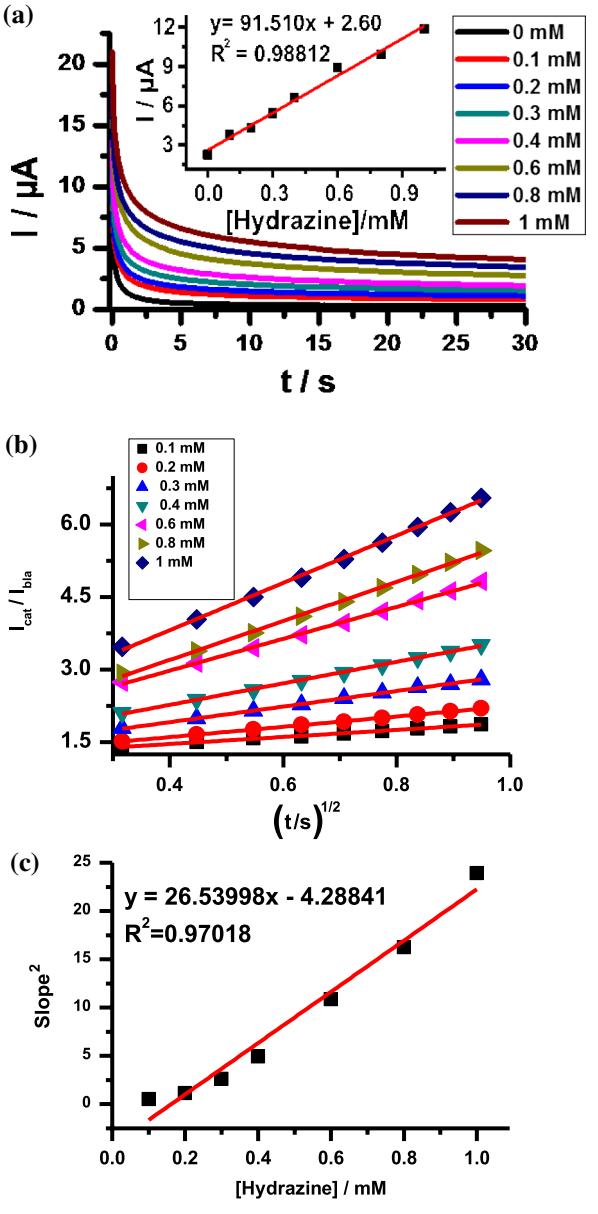

Figure 9. (a) Chronoamperograms for different concentrations of hydrazine (in 0.2 M NaOH) recorded using **3**-clicked-GCE. Insert: current-concentration plot for hydrazine. (b) Plot of (I_{cat}/I_{bla}) *vs.* $t^{1/2}$ and (c) plot of the square of the slope *vs*. concentration of hydrazine.

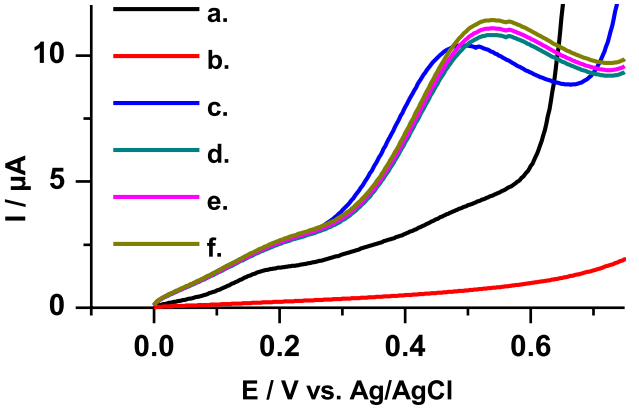

Figure 10. Square wave voltammograms in (a) 100 µM ammonia, (b) 100 µM aniline, (c) 25 µM hydrazine, (d) 25 µM hydrazine + 100 µM ammonia, (e) 25 µM hydrazine + 100 µM aniline, (*f*) 25 µM hydrazine + 100 µM aniline + 100 µM ammonia.

3.3.5. Interference studies

Amine compounds such as phenyl hydrazine, aniline and ammonia have potential to interfere with the signal of hydrazine in real life application. Hence, the selectivity of the electrode towards hydrazine in the presence of amines was studied (Figure 10). The square wave voltammograms in the presence of interferences are similar (Figure 10(d), (e), (f)), except for the small shift towards positive potentials. The peak current of hydrazine in the presence of interferences remained high enough to determine selectivity of hydrazine as the interferences produced negligible oxidation currents and no extra peak. The relative standard deviation (RSD) of the peak heights in figure 10(c), (d), (e), and (f) was 4.30%, close to RSD for hydrazine only at the clicked electrode (4.70%). Therefore, the study confirmed that the developed sensor possesses good sensitivity towards hydrazine.

4. Conclusion

The symmetrical ethynylbenzyl alkyne-terminated cobalt phthalocyanine (**3**) with high electrochemical performance was synthesized and used for electrocatalysis of hydrazine on a glassy carbon electrode modified via click reaction. The modified **3**-clicked-GC surface was characterized using cyclic voltammetry and XPS, which confirmed the success of modification steps. Electrochemical behaviors of the probe toward hydrazine displayed good catalytic rate constant and low limit of detection of 8.45×10^3 $M^{-1}s^{-1}$ and 3.28 µM, respectively.

Acknowledgements

This work was supported by the Department of Science and Technology (DST) and National Research Foundation (NRF), South Africa through DST/NRF South African Research Chairs Initiative for Professor of Medicinal Chemistry and Nanotechnology (UID 62620) as well as Rhodes University/DST Centre for Nanotechnology Innovation, Rhodes University, South Africa.

Disclosure statement

No potential conflict of interest was reported by the authors.

Funding

This work was supported by the National Research Foundation South Africa [grant number UID 62620].

References

[1] Ö.A. Osmanbaş, A. Koca, M. Kandaz, F. Karaca. *Int. J. Hydrogen Energy*, **33**, 3281 (2008).
[2] Y. Yuan, J. Ahmed, S. Kim. *J. Power Sources*, **196**, 1103 (2011).
[3] M.L. Rodriguez-Mendez, M. Luz, C. García-Hernandez, C. Medina-Plaza, C. García-Cabezón, J.A. de Saja. *J. Porphyrins Phthalocyanines*, **20**, 889 (2016).
[4] H. Wang, Y. Bu, W. Dai, K. Li, H. Wang, X. Zuo. *Sens. Actuators, B*, **216**, 298 (2015).
[5] A. Maringa, E. Antunes, T. Nyokong. *Electrochim. Acta*, **121**, 93 (2014).
[6] L. Ding, Q. Xin, X. Zhou, J. Qiao, H. Li, H. Wang. *J. Appl. Electrochem.*, **43**, 43 (2013).
[7] N. Pereira-Rodrigues, R. Cofré, J.H. Zagal, F. Bedioui. *Bioelectrochemistry*, **70**, 147 (2007).
[8] T. Nyokong. N4-macrocyclic Metal Complexes. In *Electrocatalysis, Electrophotochemistry, and Biomimetic Electrocatalysis*, J.H. Zagal, F. Bedioui, J.-P. Dodelet (Eds), pp. 315–347, Springer (2006), Chapter 7.
[9] J.P. Collman, N.K. Devaraj, C.E. Chidsey. *Langmuir*, **20**, 1051 (2004).
[10] S.R. Nxele, P. Mashazi, T. Nyokong. *Electroanalysis*, **27**, 2468 (2015).
[11] C. O'Donoghue, G. Fomo, T. Nyokong. *Electroanalysis*, **28**, 3019 (2016).
[12] S.R. Nxele, T. Nyokong. *Electrochim. Acta*, **194**, 26 (2016).
[13] C.S. O'Donoghue, M. Shumba, T. Nyokong. *Electroanalysis*, **29**, 1731 (2017).
[14] P. Wu, A.K. Feldman, A.K. Nugent, C.J. Hawker, A. Scheel, B. Voit, J. Pyun, J.M. Fréchet, K.B. Sharpless, V.V. Fokin. *Angew. Chem.*, **116**, 4018 (2004).
[15] M. Delamar, R. Hitmi, J. Pinson, J.M. Saveant. *J. Am. Chem. Soc.*, **12**, 5883 (1992).
[16] S.D. Zelnick, D.R. Mattie, P.C. Stepaniak. *Aviat. Space, Environ. Med.*, **74**, 1285 (2003).
[17] A. Umar, M.M. Rahman, S.H. Kim, Y.-B. Hahn. *Chem. Commun.*, 166 (2008).
[18] D. Evrard, F. Lambert, C. Policar, V. Balland, B. Limoges. *Chemistry*, **14**, 9286 (2008).
[19] A. Yahyazadeh, V. Azimi. *Appl. Chem.*, **49**, 9991 (2012).
[20] N. Kobayashi, H. Ogata, N. Nonaka, E.A. Luk'yanets. *Chemistry*, **17**, 5123 (2003).
[21] V.N. Nemykin, E.A. Lukyanets. *Arkivoc: J. Org. Chem.*, **136**, i (2010).
[22] E.A. Lukyanets, V.N. Nemykin. *J. Porphyrins Phthalocyanines*, **14**, 1 (2010).
[23] F. Aytan Kiliçarslan, B. Keskin, İ. Erden, A. Erdoğmuş. *J. Coord. Chem.*, **70**, 2671 (2017).
[24] K. Sakamoto, E. Ohno-Okumura. *Materials*, **2**, 1127 (2009).
[25] F. Chen, F. Wang. *Molecules*, **14**, 2656 (2009).
[26] P. Niedziałkowski, T. Ossowski, P. Zięba, A. Cirocka, P. Rochowski, S.J. Pogorzelski, J. Ryl, M. Sobaszek, R. Bogdanowicz. *J. Electroanal. Chem.*, **756**, 84 (2015).
[27] K.I. Ozoemena. *Sensors*, **6**, 874 (2006).
[28] D.A. Geraldo, C.A. Togo, J. Limson, T. Nyokong. *Electrochim. Acta*, **53**, 8051 (2008).
[29] Q.-Y. Peng, T.F. Guarr. *Electrochim. Acta*, **39**, 2629 (1994).
[30] F. Tasca, F.J. Recio, R. Venegas, D.A. Geraldo, M. Sancy, J.H. Zagal. *Electrochim. Acta*, **140**, 314 (2014).
[31] D.A. Venegas-Yazigi, G.I. Cárdenas-Jirón, J.H. Zagal. *J. Coord. Chem.*, **56**, 1269 (2003).
[32] A. Salimi, K. Abdi. *Talanta*, **63**, 475 (2004).
[33] J. Sun, Y.-H. Fang, Z.-P. Liu. *Phys. Chem. Chem. Phys.*, **16**, 13733 (2014).
[34] S. Dutta, C. Ray, S. Mallick, S. Sarkar, A. Roy, T. Pal. *RSC Adv.*, **5**, 51690 (2015).
[35] M. Coates, T. Nyokong. *Electrochim. Acta*, **91**, 158 (2013).
[36] M.A. Aziz, A.-N. Kawde. *Talanta*, **115**, 214 (2013).